Leveraging Crystal Anisotropy for Deterministic Growth of InAs Quantum Dots with Narrow Optical Linewidths

Michael K. Yakes,[†,‖] Lily Yang,[†,‡,‖] Allan S. Bracker,*[†] Timothy M. Sweeney,[†,‡] Peter G. Brereton,[†,‡,#] Mijin Kim,[§] Chul Soo Kim,[†] Patrick M. Vora,[†,‡] Doewon Park,[†] Samuel G. Carter,[†] and Daniel Gammon[†]

[†]Naval Research Laboratory, 4555 Overlook Avenue SW, Washington, D.C. 20375, United States
[§]Sotera Defense Solutions, 430 National Business Parkway, Suite 100, Annapolis Junction, Maryland 20701, United States

ABSTRACT: Crystal growth anisotropy in molecular beam epitaxy usually prevents deterministic nucleation of individual quantum dots when a thick GaAs buffer is grown over a nanopatterned substrate. Here, we demonstrate how this anisotropy can actually be used to mold nucleation sites for single dots on a much thicker buffer than has been achieved by conventional techniques. This approach greatly suppresses the problem of defect-induced line broadening for single quantum dots in a charge-tunable device, giving state-of-the-art optical linewidths for a system widely studied as a spin qubit for quantum information.

KEYWORDS: *Quantum dot, InAs, molecular beam epitaxy, site-controlled, quantum information, single photon source*
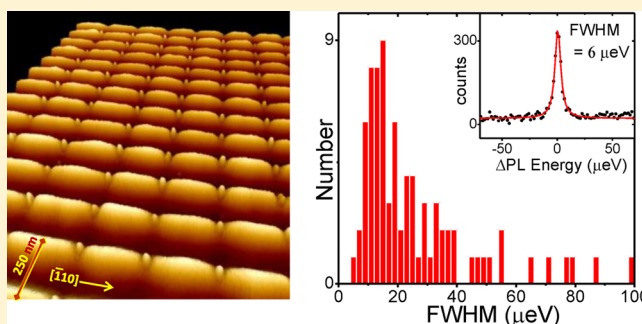
Epitaxial quantum dots (QDs) have atom-like electronic properties, including long coherence times, narrow spin-sensitive optical resonances, and large optical dipoles. This makes them attractive for single-quantum applications such as spin qubits[1–3] and single photon sources.[4,5] Epitaxial InAs QDs are usually grown by Stranski–Krastanov self-assembly, which provides considerable control over the spatial density, size, and emission wavelength of the dots. However, self-assembled dots grow at random positions on the substrate, while single-quantum device applications often require placement with sub-100 nm lateral precision. One solution is to locate individual previously grown QDs with high spatial precision and fabricate devices around them.[6,7] A more common approach, which is scalable to large networks, is to grow on a prepatterned substrate with an array of small holes that act as nucleation sites for QDs. These deterministically patterned QDs have been used as single photon emitters[8] and for studies of dot–cavity interactions.[9] The most common method for patterning the substrate is electron beam lithography followed by wet etching.[10,11] Other techniques include focused ion beam,[12,13] UV-nanoimprint lithography,[14] atomic force microscopy (AFM) oxidation,[15] and metal–organic chemical vapor deposition (MOCVD) growth on (111)B substrates without self-assembly.[9,16]

Despite the considerable promise of using prepatterned substrates to precisely position QDs in optical devices, serious technical obstacles remain. The main problem is that oxidation in air and various fabrication steps introduce a high density of impurities and intrinsic defects into the patterned GaAs surface. It is believed that charge fluctuations[17,18] at these defects produce time-dependent Stark shifts that broaden the optical resonances of nearby dots. Narrow linewidths are essential for

resolving spin fine structure, nonlinear optical effects (e.g., Autler–Townes splitting), and the vacuum Rabi splitting of strongly coupled QDs in optical cavities. Improving the linewidths of site-controlled dots has therefore been identified as an important goal by groups working in this area.[19–23]

For growths on unpatterned substrates, the problem of residual surface oxide is easily avoided by first growing a thick GaAs buffer layer (usually more than 100 nm) before the QD layer is grown. In such samples, where QDs are well-separated from defects or impurities, optical linewidths are often below 10 μeV and occasionally approach 1 μeV. In contrast, QDs grown near processed interfaces[10,20–23] or surfaces[24] show much broader linewidths, often more than 100 μeV. Another difficulty with patterned substrates for QDs is that the usual thermal deoxidation procedure for GaAs substrates causes pitting of the surface,[25] which leads to unintended nucleation of QDs. This is often addressed by using an in situ atomic hydrogen beam[10] to remove most of the oxygen and carbon from the surface and to preserve the morphology.

The requirements for precise site control and narrow optical linewidths make contradictory demands on the crystal growth process. A thick GaAs buffer improves optical linewidths, but it greatly complicates site control because growth anisotropy tends to elongate the nucleation sites. After growing a few tens of nanometers of GaAs, it becomes very difficult to nucleate individual quantum dots. This has motivated some crystal growers to use an initial layer of patterned QDs as a strain-inducing seed layer to nucleate a second (active) layer of

Report Documentation Page

1. REPORT DATE **29 AUG 2013**	2. REPORT TYPE	3. DATES COVERED **00-00-2013 to 00-00-2013**

4. TITLE AND SUBTITLE **Leveraging Crystal Anisotropy for Deterministic Growth of InAs Quantum Dots with Narrow Optical Linewidths**	5a. CONTRACT NUMBER
	5b. GRANT NUMBER
	5c. PROGRAM ELEMENT NUMBER
6. AUTHOR(S)	5d. PROJECT NUMBER
	5e. TASK NUMBER
	5f. WORK UNIT NUMBER

7. PERFORMING ORGANIZATION NAME(S) AND ADDRESS(ES) **Naval Research Laboratory,4555 Overlook Ave SW,Washington,DC,20375**	8. PERFORMING ORGANIZATION REPORT NUMBER

9. SPONSORING/MONITORING AGENCY NAME(S) AND ADDRESS(ES)	10. SPONSOR/MONITOR'S ACRONYM(S)
	11. SPONSOR/MONITOR'S REPORT NUMBER(S)

12. DISTRIBUTION/AVAILABILITY STATEMENT
Approved for public release; distribution unlimited

13. SUPPLEMENTARY NOTES

14. ABSTRACT
Crystal growth anisotropy in molecular beam epitaxy usually prevents deterministic nucleation of individual quantum dots when a thick GaAs buffer is grown over a nanopatterned substrate. Here, we demonstrate how this anisotropy can actually be used to mold nucleation sites for single dots on a much thicker buffer than has been achieved by conventional techniques. This approach greatly suppresses the problem of defect-induced line broadening for single quantum dots in a charge-tunable device, giving state-of-the-art optical linewidths for a system widely studied as a spin qubit for quantum information.

15. SUBJECT TERMS

16. SECURITY CLASSIFICATION OF:			17. LIMITATION OF ABSTRACT	18. NUMBER OF PAGES	19a. NAME OF RESPONSIBLE PERSON
a. REPORT **unclassified**	b. ABSTRACT **unclassified**	c. THIS PAGE **unclassified**	**Same as Report (SAR)**	**6**	

dots,[8,20] thereby extending the total thickness of the buffer. This technique has recently been combined with rigorous cleaning of the processed surface to demonstrate QDs with the best optical linewidths to date.[19]

In this work, we describe a method of growing individual site-controlled QDs and short QD chains of controllable length on GaAs buffer layers of at least 90 nm, without a QD seed layer and without the requirement for atomic hydrogen cleaning. Because we are able to grow these dots far away from the patterned interface, we have measured optical linewidths as low as 6 μeV. The GaAs growth anistropy, instead of being a problem, is actually the reason that this method works.

The problem that the GaAs growth anisotropy usually presents for site-controlled InAs QD growth is demonstrated in Figure 1. Figure 1a shows QDs grown on etched nanoholes
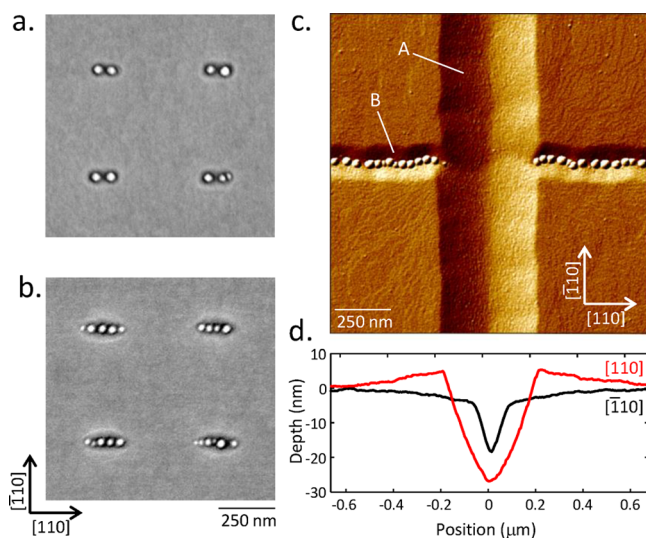

Figure 1. (a) InAs quantum dots on a hole-patterned substrate with a 12 nm GaAs buffer overgrowth (SEM image). (b) InAs dots on a hole-patterned substrate covered with a 30 nm GaAs buffer overgrowth. (c) InAs dots on a crossed line-patterned substrate covered with a 90 nm GaAs buffer (AFM phase image). Quantum dots grow only in [110] lines with arsenic-terminated B-steps, not in [$\bar{1}$10] lines with gallium-terminated A-steps. (d) Plot of [110] and [$\bar{1}$10] cross-section profiles of the lines in panel c. Cross-sections prior to growth would be similar to those shown in Figure 2d, first panel.

covered by a 12 nm GaAs buffer. During the buffer growth, the holes widen along [110], and pairs of QDs nucleate. With thin buffers (<20 nm), it is possible to nucleate individual dots under the appropriate growth conditions, but this becomes much less probable as the buffer thickness is increased. Figure 1b shows dots grown on a 30 nm thick buffer, where the holes are further elongated and chains of QDs form.

This growth anisotropy results from a combination of factors that includes incorporation chemistry on vicinal surfaces, gallium atom diffusion on and between facets, and the structure of the initially etched lines.[26,27] The incorporation anisotropy is believed to originate in part from the chemical inequivalence of atomic step edges running in [$\bar{1}$10] and [110] crystal directions.[26,28,29] Gallium adatoms incorporate more easily at arsenic-terminated B-steps (along [110]) than at gallium-terminated A-steps (along [$\bar{1}$10]). As the etched features grow, they form faceted sidewalls[11] that have predominantly A or B type steps, and there is a net movement of gallium adatoms

away from A-stepped facets to more favorable positions on B-steps or on the flat (001) surface. This leads to the widening of features in the [110] direction. In the [$\bar{1}$10] direction, we find that patterned features can expand or contract, depending on the growth conditions. This behavior is similar to the GaAs growth kinetics observed on (001) patterned substrates with (111)A and (111)B facets.[30−32]

The effect of growth anisotropy on etched lines is shown in Figure 1c, where we started with an etched pattern of crossed lines (~30 nm deep and 80 nm wide). Prior to growth, the lines had cross-sections similar to those shown in the first panel of Figure 2d. After reintroducing the patterned substrate into the MBE chamber, we grew 90 nm of GaAs. The [110] line with B-step sidewalls is still narrow, while the [$\bar{1}$10] line has widened dramatically with A-stepped sidewalls sloped at roughly 10 degrees. The GaAs surface next to the [$\bar{1}$10] ([110]) line shows a shallow accumulation (depletion) region, seen in the cross-section profiles of Figure 1d.[31,32] When InAs is deposited on the surface at just below the critical thickness for QD growth on a flat surface, we observe QDs in the narrow [110] line but not in the wide [$\bar{1}$10] line.[15,33,34] Notably, the sloped sidewalls of the [$\bar{1}$10] line are barely affected by the intersection with the [110] line, and no dots nucleate at the intersection.

This growth evolution of the etched lines presents a highly favorable situation for nucleating a controllable number of dots. The concept is depicted in Figure 2a. A row of holes is patterned between [$\bar{1}$10] lines in the GaAs substrate (gray). Typical dimensions for these features are 80 nm wide and 30 nm deep, as shown in the first AFM image of Figure 2c. When a thick buffer (blue) is grown on this pattern, both holes and lines widen along [110]. As the lines widen, they truncate the elongation of the holes, leaving notches at the top of a ridge between the broadened lines. Each notch is a short [110] line segment that serves as a nucleation site for QDs. The number of QDs that can fit in each site is determined by its width, which is directly controllable through the line spacing (d), the GaAs buffer thickness (t), and the growth conditions.

With multiple periods of etched lines and holes, an array of individual QDs with highly uniform morphology can be grown on a thick GaAs buffer separating the dots from the original etched pattern. Figure 2b shows an example of dots grown on a buffer of thickness t = 90 nm and line spacing of d = 250 nm (the vertical scale is expanded for clarity). Figure 2c shows the effect of increasing the line spacing, with short chains of QDs forming in each site. As the spacing d increases from 240 nm to 280 nm and 320 nm, each site nucleates predominantly one, two, or three dots, respectively. The growth statistics in Figure 2f were produced by counting roughly 240 nucleation sites for each line spacing. The single QD uniformity demonstrated for a 90 nm GaAs buffer here is comparable to other work using round hole nucleation sites covered by GaAs buffer layers of only 10 nm.[10] We note that the examples shown in Figure 2 were treated with atomic hydrogen prior to growth, and while they are the best we have observed so far, we have also observed single QD uniformity up to 70% on similar samples with a thermally desorbed oxide.

The important features of the patterned substrate morphology are clarified with line profiles of the images in Figure 2c. Line profiles parallel to [110] cut across the etched lines (Figure 2d), while profiles parallel to [$\bar{1}$10] cut across the nucleation sites and dots at the top of the ridges (Figure 2e). The dot count is correlated with the width of the notches. The postgrowth profiles show that three (or more) dots nucleate
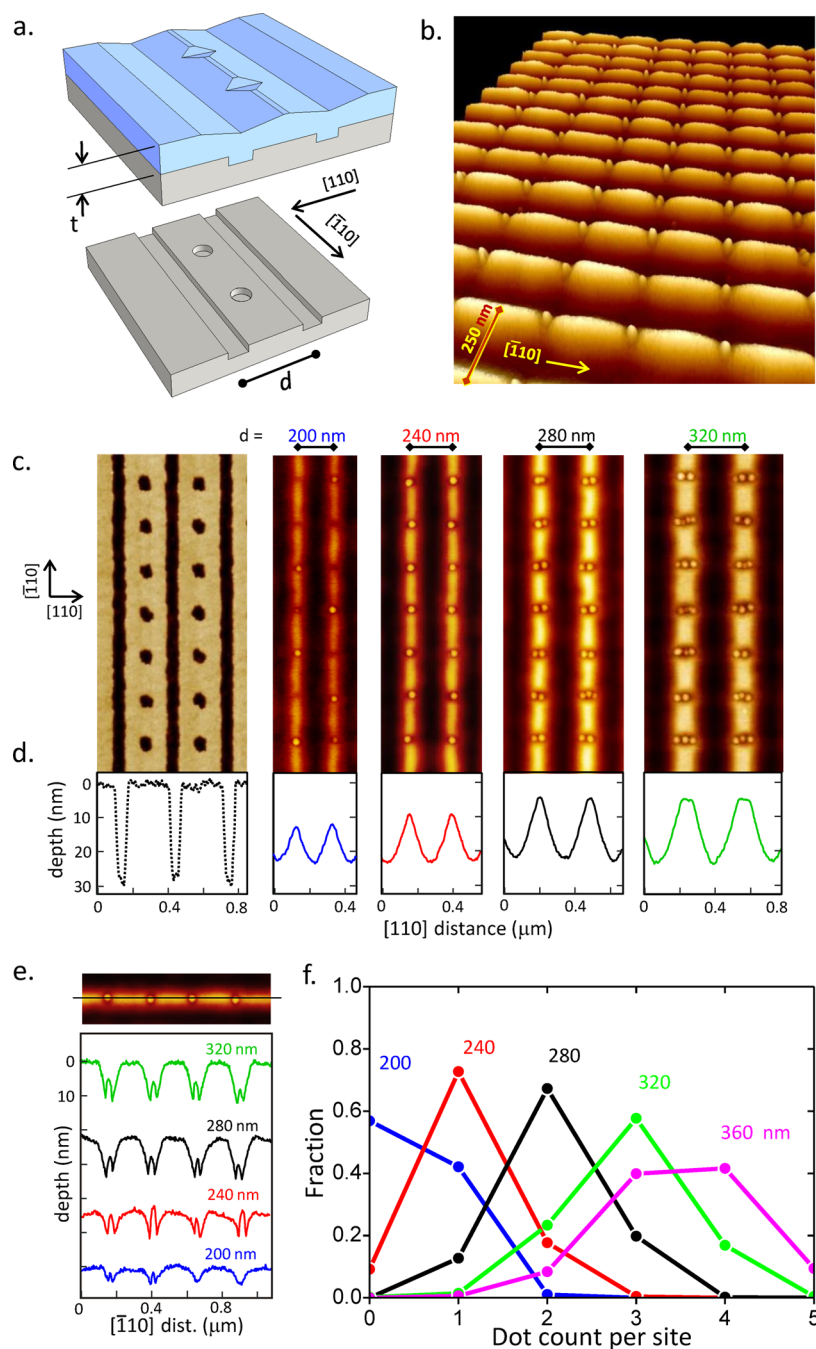
Figure 2. (a) Perspective of patterned substrate before buffer growth (lower) and after buffer growth (upper) (substrate is gray, buffer is blue). Lateral and vertical dimensions are shown with equal scaling, corresponding to a realistic structure. (b) Perspective (AFM image) of individual quantum dots grown on a pattern with $d = 250$ nm line spacing and $t = 90$ nm GaAs buffer thickness. The z dimension is expanded with respect to x and y dimensions for clarity. (c) AFM images of QDs grown on patterned substrate with several values of the line spacing, d. (Left side shows typical substrate pattern before GaAs buffer growth.) (d) Cross-section profiles of images in panel c along [110], between the nucleation sites. (Sidewall profiles in first panel are AFM resolution-limited.) (e) Cross-section profiles of images in panel c along [$\bar{1}$10] at the top of the ridge and through the nucleation sites. (f) Distributions of dot count per nucleation site; $N \approx 240$ sites for each value of d.

when a flat plateau remains between adjacent [$\bar{1}$10] lines ($d = 320$ nm), and when the plateau is nearly eliminated ($d = 280$ nm), two dots form. Single dot nucleation occurs when the plateau between the lines has been eliminated, and the remaining ridge has been reduced in height from 18 nm to about 13 nm. For $d = 240$ nm, the depth of the nucleation sites has also begun to shrink below 10 nm (Figure 2e). Nucleation is incomplete for the smallest line spacing ($d = 200$ nm), where the nucleation sites are less than 5 nm deep.

In order to test the optical and electronic quality of these QDs, we incorporated site-controlled QDs into a Schottky diode heterostructure that allows injection of individual electrons into each QD and performed single QD photo-luminescence spectroscopy as a function of applied bias. The patterned surface was buried in the n-type region of the Schottky diode, and the thickness of the n-type region above the dots was adjusted to make the total buffer thickness 90 nm (Figure 3a). The photoluminescence spectrum as a function of
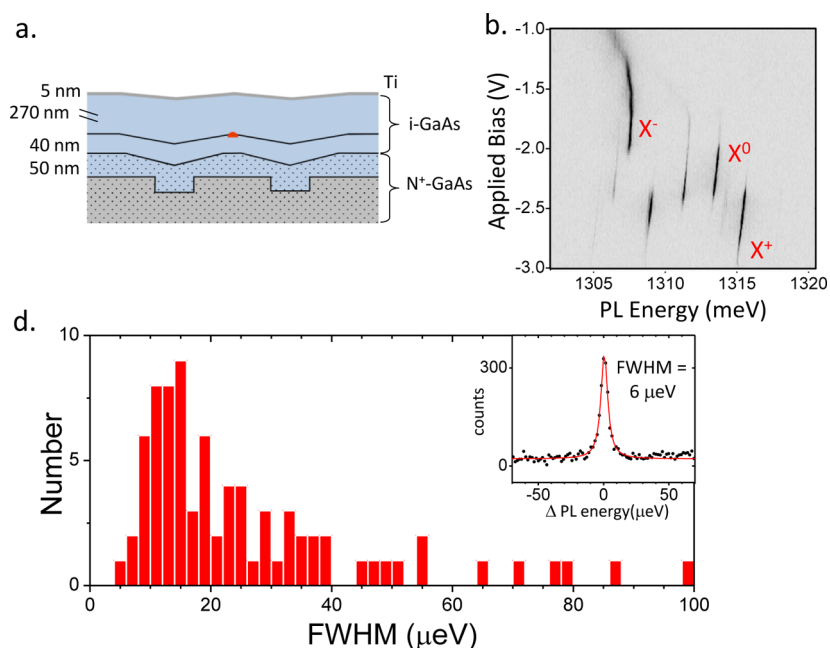
Figure 3. (a) Schematic of the Schottky diode heterostructure, indicating the patterned substrate (gray) and the overgrown GaAs buffer and capping layer (blue). Lateral and vertical dimensions are shown with equivalent scaling, corresponding to a realistic structure. (b) Photoluminescence intensity (gray scale) as a function of PL energy and applied bias. Neutral exciton (X^0), positive (X^+), and negative (X^-) trions are indicated. (c) Distribution of linewidths for 80 PL lines from dots grown in high density arrays such as those in Figure 2b,c; inset, PL line of an individual quantum dot.

applied bias (Figure 3b) shows a typical charging sequence for single dots, with optical transitions for neutral (X^0), negatively charged (X^-), and positively charged (X^+) excitons. Other lines originate from biexciton complexes. This is a standard fingerprint for InAs self-assembled dots; however, the range of applied bias over which these transitions are observed is considerably more negative than for unpatterned samples. For example, the transition from X^0 to X^-, which occurs here at −2 V, is typically observed at a positive bias in unpatterned QD Schottky diode samples with similar layer thicknesses. This offset indicates that the electric field profile of our Schottky diode is different than for unpatterned samples, implying the presence of additional charges within the structure. Our best samples for PL studies were not treated with atomic hydrogen for GaAs deoxidation prior to growth because we have observed even larger offsets in hydrogen-treated samples. We have not yet incorporated the atomic hydrogen source directly into the molecular beam epitaxy (MBE) growth chamber, which may yet lead to a reduction in interface defects when the atomic hydrogen is used.

Despite the presence of processing defects, the photoluminescence linewidths of the site-controlled dots are very narrow. To resolve the linewidths, we used a scanning Fabry−Perot etalon with an energy resolution of ~1.5 μeV as an energy filter in front of a standard grating spectrometer.[35,36] In order to obtain sufficient statistics, we measured a large number of dots in dense arrays such as those shown in Figure 2b,c. Because of the large density of spectral lines, we were unable to assign every line to a specific excitonic species, although some showed clear anisotropic exchange doublets associated with neutral excitons. Figure 3c shows a histogram of measured linewidths for roughly 80 measured spectral lines. The linewidths range between 6 and 100 μeV with a median of 19 μeV, which is approaching the linewidths for unpatterned QD diode samples from our laboratory. The observed range is

much lower than what has been reported in most examples of site-controlled dots to date. We believe that the primary reason for the improvement in optical linewidths here is the thick GaAs buffer layer separating the QDs from the processed interface. We note that the n-doped conducting buffer surrounding the patterned interface may serve to electrically screen the fluctuations of charged defects, and a systematic study of the effect of heterostructure design would help to isolate a contribution from this effect to the observed linewidths.

The results described here were obtained with a 90 nm GaAs buffer, but we anticipate that it will be possible to work with considerably thicker buffers. With more GaAs, the small nucleation sites may fill in under the present growth conditions, but this can be prevented by changing the dimensions of the substrate pattern or by changing the growth temperature or arsenic flux to influence the growth anisotropy. With no optimization, we are already able to nucleate ~50% single dots on a 120 nm buffer by starting with a deeper etch (60 nm). We also note that the uniformity of the nucleation sites is quite sensitive to the surface preparation that precedes the wet etch. After development of the ebeam resist, we use a brief oxygen plasma or UV−ozone exposure to remove resist residue from the GaAs surface. This produces much smoother postetch surfaces (1−3 nm roughness) on the bottom and sides of the etched features compared to without oxidation (5−10 nm roughness).

By using MBE on nanoengineered GaAs substrates, we have grown deterministically positioned InAs quantum dots with nearly intrinsic linewidths. The key to our approach is to harness the usually problematic GaAs anisotropy to grow thick protective buffers between the dots and the patterned surface, while still nucleating dots with a high degree of uniformity. We believe that still thicker GaAs buffers can be grown without sacrificing uniformity by further optimizing the substrate

pattern fabrication and growth conditions and that deterministic nucleation of epitaxial InAs quantum dots with intrinsic optical quality is within reach. This removes a major obstacle toward sophisticated quantum dot complexes such as a quantum network of spin qubits.

Methods. *Substrate Patterning.* Lines and circles were patterned by electron beam lithography in 70 nm PMMA resist. The electron beam (25 kV; 10 μm aperture) had doses ranging from 1000 to 2500 pC/cm adjusted according to feature density. The resist was developed in 1:3 MIBK/IPA for 90 s. Prior to etching, a two minute UV−ozone exposure was used to remove residual resist and resulted in smoother etched lines. Samples were etched at ∼0.5 nm/s in $H_3PO_4/H_2O_2/H_2O$ (1:4:495). The resist was removed in standard heated solvents and remover and a brief UV−ozone treatment. The resulting features were 60−90 nm wide.

Sample Growth. Quantum dot samples were grown by molecular beam epitaxy. The patterned substrate was rinsed in 10% HCl and water to remove surface oxide immediately prior to loading. The remaining oxide was removed either by atomic hydrogen in a separate chamber or thermally (∼620 °C) under arsenic vapor in the MBE growth chamber. The choice of oxide removal technique had little effect on the surface morphology. A 50 nm silicon-doped (3×10^{18} cm^{-3}) GaAs buffer layer was grown at 0.7 ML/s at 550 °C, followed by a 40 nm intrinsic GaAs layer. The temperature was reduced to 520 °C for QD growth. InAs was deposited over 60 s, to within a few percent of the critical thickness for QD formation on unpatterned regions of the substrate. For PL samples, the QD was truncated to 2.8 nm with the indium flush technique to give PL energies around 950 nm, followed by an additional 280 nm of intrinsic GaAs. Temperatures were measured with band-edge thermometry.

Photoluminescence Measurements. Patterned QDs were incorporated into a Schottky diode heterostructure as shown in Figure 3a. A 5 nm semitransparent titanium layer was used as a top contact. Measurements were done in a continuous flow helium cryostat at ∼8 K. PL was excited and collected through a microscope objective and resolved in a single grating spectrometer. For high spectral resolution, the PL was filtered with a scanning Fabry−Perot etalon prior to entering the spectrometer. The etalon consisted of one planar and one curved mirror separated by a ring-shaped piezoelectric (PZT) crystal and had a linewidth of 1.5 μeV (FWHM). Peaks were measured at applied biases below the X$^-$ charging transition, where mostly X^0, X$^+$, and some biexciton peaks are observed.

■ AUTHOR INFORMATION

Corresponding Author
*(A.S.B.) E-mail: bracker@nrl.navy.mil. Phone: (202) 404-4523. Fax: (202) 767-1165.

Present Address
#Department of Physics, US Naval Academy, 572c Holloway Road, Annapolis, MD 21401, United States.

Author Contributions
||M.K.Y. and L.Y. contributed equally to this work.

Notes
The authors declare no competing financial interest.
‡National Research Council Postdoctoral Research Associate, residing at the Naval Research Laboratory.

■ REFERENCES

(1) Liu, R. B.; Yao, W.; Sham, L. J. *Adv. Phys.* **2010**, *59*, 703−802.
(2) Kim, D.; Carter, S. G.; Greilich, A.; Bracker, A. S.; Gammon, D. *Nat. Phys.* **2011**, *7*, 223−229.
(3) Press, D.; Ladd, T. D.; Zhang, B. Y.; Yamamoto, Y. *Nature* **2008**, *456*, 218−221.
(4) Michler, P.; Kiraz, A.; Becher, C.; Schoenfeld, W. V.; Petroff, P. M.; Zhang, L. D.; Hu, E.; Imamoglu, A. *Science* **2000**, *290*, 2282−2285.
(5) Shields, A. J. *Nat. Photonics* **2007**, *1*, 215−223.
(6) Badolato, A.; Hennessy, K.; Atature, M.; Dreiser, J.; Hu, E.; Petroff, P. M.; Imamoglu, A. *Science* **2005**, *308*, 1158−1161.
(7) Dousse, A.; Lanco, L.; Suffczynski, J.; Semenova, E.; Miard, A.; Lemaitre, A.; Sagnes, I.; Roblin, C.; Bloch, J.; Senellart, P. *Phys. Rev. Lett.* **2008**, *101*, 267404.
(8) Schneider, C.; Heindel, T.; Huggenberger, A.; Weinmann, P.; Kistner, C.; Kamp, M.; Reitzenstein, S.; Hoefling, S.; Forchel, A. *Appl. Phys. Lett.* **2009**, *94*, 111111.
(9) Calic, M.; Gallo, P.; Felici, M.; Atlasov, K. A.; Dwir, B.; Rudra, A.; Biasiol, G.; Sorba, L.; Tarel, G.; Savona, V.; Kapon, E. *Phys. Rev. Lett.* **2011**, *106*, 227402.
(10) Atkinson, P.; Schmidt, O. G.; Bremner, S. P.; Ritchie, D. A. *C. R. Phys.* **2008**, *9*, 788−803.
(11) Heidemeyer, H.; Muller, C.; Schmidt, O. G. *J. Cryst. Growth* **2004**, *261*, 444−449.
(12) Mehta, M.; Reuter, D.; Wieck, A. D.; de Vasconcellos, S. M.; Zrenner, A.; Meier, C. *Appl. Phys. Lett.* **2010**, *97*, 143101.
(13) Lee, J.; Saucer, T. W.; Martin, A. J.; Tien, D.; Millunchick, J. M.; Sih, V. *Nano Lett.* **2011**, *11*, 1040−1043.
(14) Schramm, A.; Tommila, J.; Strelow, C.; Hakkarainen, T. V.; Tukiainen, A.; Dumitrescu, M.; Mews, A.; Kipp, T.; Guina, M. *Nanotechnology* **2012**, *23*, 175701.
(15) Martin-Sanchez, J.; Alonso-Gonzalez, P.; Herranz, J.; Gonzalez, Y.; Gonzalez, L. *Nanotechnology* **2009**, *20*, 125302.
(16) Juska, G.; Dimastrodonato, V.; Mereni, L. O.; Gocalinska, A.; Pelucchi, E. *Nat. Photonics* **2013**, *7*, 527−531.
(17) Houel, J.; Kuhlmann, A. V.; Greuter, L.; Xue, F.; Poggio, M.; Gerardot, B. D.; Dalgarno, P. A.; Badolato, A.; Petroff, P. M.; Ludwig, A.; Reuter, D.; Wieck, A. D.; Warburton, R. J. *Phys. Rev. Lett.* **2012**, *108*, 107401.
(18) Robinson, H. D.; Goldberg, B. B. *Phys. Rev. B* **2000**, *61*, R5086−R5089.
(19) Jons, K. D.; Atkinson, P.; Muller, M.; Heldmaier, M.; Ulrich, S. M.; Schmidt, O. G.; Michler, P. *Nano Lett.* **2013**, *13*, 126−130.
(20) Pfau, T. J.; Gushterov, A.; Reithmaier, J. P.; Cestier, I.; Eisenstein, G.; Linder, E.; Gershoni, D. *Appl. Phys. Lett.* **2009**, *95*, 243106.
(21) Skiba-Szymanska, J.; Jamil, A.; Farrer, I.; Ward, M. B.; Nicoll, C. A.; Ellis, D. J. P.; Griffiths, J. P.; Anderson, D.; Jones, G. A. C.; Ritchie, D. A.; Shields, A. J. *Nanotechnology* **2011**, *22*, 065302.
(22) Huggenberger, A.; Heckelmann, S.; Schneider, C.; Hoefling, S.; Reitzenstein, S.; Worschech, L.; Kamp, M.; Forchel, A. *Appl. Phys. Lett.* **2011**, *98*, 131104.
(23) Faure, S.; Nishioka, M.; Ishida, S.; Guimard, D.; Arakawa, Y. *Appl. Phys. Express* **2011**, *4*, 112001.
(24) Wang, C. F.; Badolato, A.; Wilson-Rae, I.; Petroff, P. M.; Hu, E.; Urayama, J.; Imamoglu, A. *Appl. Phys. Lett.* **2004**, *85*, 3423−3425.
(25) Lee, J. J. D.; West, K. W.; Baldwin, K. W.; Pfeiffer, L. N. *J. Cryst. Growth* **2012**, *356*, 46−52.

(26) Shitara, T.; Vvedensky, D. D.; Wilby, M. R.; Zhang, J.; Neave, J. H.; Joyce, B. A. *Phys. Rev. B* **1992**, *46*, 6825−6833.

(27) Pelucchi, E.; Dimastrodonato, V.; Rudra, A.; Leifer, K.; Kapon, E.; Bethke, L.; Zestanakis, P. A.; Vvedensky, D. D. *Phys. Rev. B* **2011**, *83*, 205409.

(28) Bell, G. R.; Jones, T. S.; Joyce, B. A. *Surf. Sci.* **1999**, *429*, L492−L496.

(29) Horikoshi, Y.; Yamaguchi, H.; Briones, F.; Kawashima, M. *J. Cryst. Growth* **1990**, *105*, 326−338.

(30) Hata, M.; Isu, T.; Watanabe, A.; Katayama, Y. *J. Vac. Sci. Technol., B* **1990**, *8*, 692−696.

(31) Shen, X. Q.; Kishimoto, D.; Nishinaga, T. *Jpn. J. Appl. Phys., Part 1* **1994**, *33*, 11−17.

(32) Shiraishi, K.; Suzuki, Y. Y.; Kageshima, H.; Ito, T. *Appl. Surf. Sci.* **1998**, *130*, 431−435.

(33) Kohmoto, S.; Nakamura, H.; Ishikawa, T.; Nishikawa, S.; Nishimura, T.; Asakawa, K. *Mater. Sci. Eng., B* **2002**, *88* (2−3), 292−297.

(34) Heidemeyer, H.; Muller, C.; Schmidt, O. G. *J. Cryst. Growth* **2004**, *261* (4), 444−449.

(35) Metcalfe, M.; Muller, A.; Solomon, G. S.; Lawall, J. *J. Opt. Soc. Am. B* **2009**, *26*, 2308−2314.

(36) Muller, A.; Flagg, E. B.; Lawall, J. R.; Solomon, G. S. *Opt. Lett.* **2010**, *35*, 2293−2295.